

The effect of Si doping on the defect structure of GaN/AlN/Si(111)

S. I. Molina,^{a)} A. M. Sánchez, F. J. Pacheco, and R. García

Departamento de Ciencia de los Materiales e Ingeniería Metalúrgica y Química Inorgánica, Universidad de Cádiz, 11510 Puerto Real, Cádiz, Spain

M. A. Sánchez-García, F. J. Sánchez, and E. Calleja

Departamento de Ingeniería Electrónica, ETSI Telecomunicación, UPM, Ciudad Universitaria, s/n 28040 Madrid, Spain

(Received 4 January 1999; accepted for publication 8 April 1999)

The effect of Si doping on the structural quality of wurtzite GaN layers grown by molecular beam epitaxy on AlN buffered (111) Si substrates is studied. The planar defect density in the grown GaN layer strongly increases with Si doping. The dislocation density at the free surface of GaN significantly decreases when Si doping overpasses a limit value. Si doping affects the misorientation of the subgrains that constitutes the mosaic structure of GaN. The increase of the planar defect density and out-plane misorientation angles of the GaN subgrains with Si doping explain the decrease of dislocations that reach the free surface of GaN. A redshift in the photoluminescence spectra together with a decrease in the *c*-axis lattice parameter as the Si doping increases point to an increase in the residual biaxial tensile strain in the GaN samples. © 1999 American Institute of Physics. [S0003-6951(99)04222-9]

The epitaxial growth of GaN on Si is of particular interest because the Si technology is well established and GaN has attractive optoelectronic, high power and high-temperature electronic properties. The work on GaN heteroepitaxy on other substrates, such as sapphire and SiC is abundant, unlike the GaN heteroepitaxy on Si(111) that has received less attention although several reports have already been published^{1,2} where an AlN buffer layer was found to improve the GaN quality.² On the other hand, the incorporation of Si in GaN has been studied both in heteroepitaxies on Si,³ and other substrates such as sapphire,^{4,5} where it was found to improve the layer quality.⁵ In this work we determine the effect of the Si incorporation on the structural quality of GaN layers grown by molecular beam epitaxy (MBE) on AlN buffered (111) Si substrates. The mechanisms that lead to a reduction of dislocations at the free surface with increasing concentration of Si will be studied.

A series of undoped and Si-doped GaN films have been grown by plasma-assisted MBE on *p*-type resistive ($>100\ \Omega\ \text{cm}$) Si(111) on axis substrates. An optimized AlN buffer layer^{3,6,7} has been grown on the Si substrate before the GaN growth. The GaN layers were grown at 760 °C with thicknesses around 0.8 μm . A detailed explanation of the growth system and substrate preparation have been published elsewhere.⁷ This work focuses on three types of samples: (i) undoped samples that will be labeled as N0, (ii) low Si doping, $n_{\text{Si}}=1.1\times 10^{17}\ \text{cm}^{-3}$ (sample N17), and (iii) high Si doping, $n_{\text{Si}}=6.0\times 10^{18}\ \text{cm}^{-3}$ (sample N18).

Samples have been studied by transmission electron microscopy (TEM) and associated techniques. Preparation of these specimens was performed by mechanical thinning and ion milling. The TEM study was carried out with both cross sectional TEM (XTEM) and plan view TEM (PVTEM) orientations with the TEMs Jeol 1200 EX and 2000 EX for the

high resolution electron microscopy (HREM) work. Low-temperature photoluminescence (PL) was performed with the 334 nm line of an Ar⁺ laser using a Jobi-Yvon THR 1000 monochromator and detected with an ultraviolet (UV)-enhanced GaAs photomultiplier and a lock-in amplifier.

The TEM and selected area electron diffraction (SAED) studies of the epilayer show that GaN has an hexagonal structure oriented with its [11–20] direction parallel to the Si [110] direction being the GaN [0001] growth direction parallel to the Si [111] direction. The GaN layer, as deduced from PVTEM and XTEM observations, consists of a mosaic structure where subgrains are slightly misoriented. The PVTEM image of Fig. 1 shows the defect and grain distributions of the GaN layer in sample N0. The appearance of the PVTEM images in Si doped samples (N17 and N18) is similar to that shown in Fig. 1, although the average grain size is smaller with respect to the undoped sample.⁸ The analysis of PVTEM images recorded under weak beam conditions permits us to obtain the density of dislocations that reach the free surface of the grown GaN layer. Table I summarizes the dislocation density measured in the three samples studied after analyzing a region that contains hundreds of grains. There is a clear reduction in the measured dislocation density as the Si doping increases. The mechanisms that lead to this reduction will be explained below. The dislocations considered for the measured density ρ_D are those with Burgers vectors $b=1/3\langle 11-20\rangle$ and $b=1/3\langle 11-23\rangle$. It is worth noting that edge dislocations are the main dislocation type observed in GaN heteroepitaxies, while screw dislocations are greatly reduced during growth through half loop formations.⁹

The GaN layers present other structural defects: (i) planar defects in the (0001) growth plane and (ii) inversion boundaries that propagate vertically along the [0001] growth direction. Diffraction contrast $\mathbf{g}\cdot\mathbf{R}$ analysis lets us determine that these planar defects consist of stacking faults on the

^{a)}Electronica mail: sergio@molina@uca.es

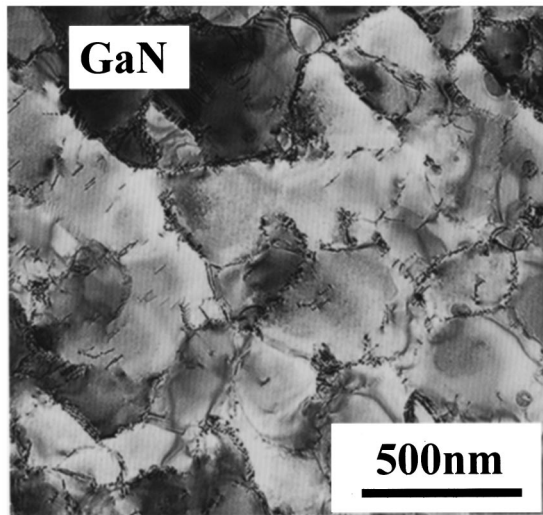


FIG. 1. Bright field PVTEM image of the GaN layer of the undoped sample recorded under two beams condition for $g = (11-20)$.

wurtzite basal plane. By HREM it is evidenced that such stacking faults usually are stacked along the $[0001]$ growth direction at distances on the order of 10 nm. The planar defect density clearly increases as the Si doping increases. Its value is $0.6 \mu\text{m}^{-1}$ for the undoped sample and it increases up to $4.0 \mu\text{m}^{-1}$ in sample N18 ($n_{\text{Si}} = 6.0 \times 10^{18} \text{cm}^{-3}$). An opposite tendency is observed for inversion domains. The inverted domains were determined using the procedure followed by Romano *et al.*¹⁰ that uses multiple dark field TEM images with $g = \pm(0002)$ along a noncentrosymmetric axis. To confirm the existence of such inverted domains, two beam images taken with $g = (1-100)$ near the $[11-20]$ zone were analyzed.¹¹

The subgrains that configure the mosaic structure of GaN are slightly misoriented both in- and out-plane (0001) growth. By analyzing electron microdiffraction patterns recorded from adjacent subgrains in plan view and cross section prepared specimens, it was possible to measure the out-plane misorientation between subgrains to be $2.0^\circ \pm 0.5^\circ$ in the Si doped samples studied. This value is larger than that measured in the undoped sample that resulted in $1.0^\circ \pm 0.5^\circ$.

The distribution of misorientations in the subgrains constituting the mosaic structure and the density of planar defects are decisive to explain the reduction in the dislocation density observed in the different samples (Table I). The density of planar defects is clearly larger as the Si doping increases. It is observed by TEM that the interaction of these planar defects, located on the (0001) planes, with the vertical line dislocations contributes to the decrease in the number of vertical dislocations that reach the free surface of the GaN layer. Similar interactions of threading dislocations that terminate on (0001) planar defects have been observed in GaN layers grown by metalorganic chemical vapor deposition (MOCVD) on sapphire.^{12,13} The increase in the measured out-plane misorientation with the Si doping may also lead to an increment in the number of dislocations which have lines perpendicular to the $[0001]$ growth direction, promoting interactions with the dislocations which propagate with their lines vertically along the growth direction. These arguments explain the decrease in the dislocation density measured at

TABLE I. Dislocation densities ρ measured from PVTEM images recorded under weak beam conditions in undoped (N0) and doped (N17 and N18) samples.

Sample	N0	N17	N18
ρ_D (cm^{-2})	$6.4 \pm 0.5 \times 10^9$	$5.3 \pm 0.5 \times 10^9$	$8 \pm 2 \times 10^8$

the free surface of the GaN layer as the Si doping level increases (Table I). These ideas also explain the results of Ruvimov *et al.*⁵ that observed a bending of the threading dislocations into the basal plane to become segments of misfit dislocations parallel to the interface.

Figure 2 shows the low-temperature PL spectra and the value of the c -axis lattice constant measured by x-ray diffraction (XRD) of the Si-doped GaN samples (N17 and N18) and the undoped reference one (N0). The increase of the PL spectra intensity with Si doping suggests that such emission is related to Si donors. The fact that this emission is also present in the undoped sample can be explained due to a Ga/Si interdiffusion process taking place at the GaN/Si(111) interfaces as is confirmed by secondary ion mass spectrometry data.¹⁴ It can be seen that the peak at around 3.45 eV redshifts while the c -axis lattice parameter decreases as the Si doping density increases. Both results point to an enhancement of the biaxial tensile strain with increasing Si doping. The reduction in the dislocation density, previously observed by TEM techniques, can also be correlated with these findings.

We conclude that the Si doping level of a GaN layer grown by MBE on (111) Si substrates determines the structural quality of the grown GaN layer. Densities of dislocations and inverted domains at the free surface of the grown layer are found to decrease with the Si doping, while the density of planar defects within the GaN layer follows an opposite trend. Misorientations between the subgrains that form the mosaic structure of the grown GaN layer and the planar defect density clearly depend on the Si density and explain the quality of improvement in the GaN layers studied by Si doping. A decrease of one order of magnitude in the threading dislocation density is achieved by doping with Si

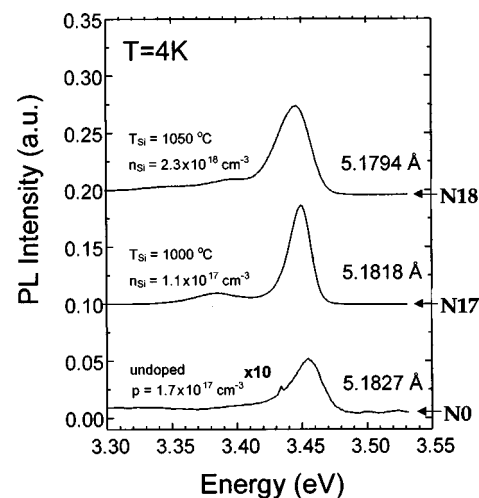


FIG. 2. Low-temperature PL spectra of the Si-doped GaN layers (N17 and N18) and the undoped one (N0). On the right side: values of the c -axis lattice constant from XRD data.

to $6 \times 10^{18} \text{ cm}^{-3}$. A redshift in the PL spectra, together with a decrease in the *c*-axis lattice parameter, point to an increase in the residual biaxial tensile strain in the GaN samples as the Si doping increases. This is in agreement with the previous results obtained by TEM techniques.

This work has been supported by CICYT Project No. MAT98-0823-C03-02 and Junta de Andalucía (Group No. PAI TEP 0120). The group from Madrid wishes to acknowledge the financial support provided by Project No. EU ESPRIT LTR 20968 (Laquani).

¹A. Ohtani, K. S. Stevens, and R. Beresford, *Appl. Phys. Lett.* **65**, 61 (1994).

²W. J. Meng and T. A. Perry, *J. Appl. Phys.* **76**, 7824 (1994).

³M. A. Sánchez-García, E. Calleja, F. J. Sánchez, F. Calle, E. Monroy, D. Basak, E. Muñoz, C. Villar, A. Sanz-Hervás, M. Aguilar, J. J. Serrano, and J. M. Blanco, *J. Electron. Mater.* **27**, 276 (1998).

⁴I.-H. Lee, I.-H. Choi, C. R. Lee, and S. K. Noh, *Appl. Phys. Lett.* **71**, 1359 (1997).

⁵S. Ruvimov, Z. Liliental-Weber, T. Suski, J. W. Ager III, J. Washburn, J. Krueger, C. Kisielowski, E. R. Weber, H. Amano, and I. Akasaki, *Appl. Phys. Lett.* **69**, 990 (1996).

⁶E. Calleja, M. A. Sánchez-García, E. Monroy, F. J. Sánchez, E. Muñoz, A. Sanz-Hervás, C. Villar, and M. Aguilar, *J. Appl. Phys.* **82**, 4681 (1997).

⁷M. A. Sánchez-García, E. Calleja, E. Monroy, F. J. Sánchez, F. Calle, E. Muñoz, and R. Beresford, *J. Cryst. Growth* **183**, 23 (1998).

⁸S. I. Molina, A. M. Sánchez, F. J. Pacheco, R. García, M. A. Sánchez-García, and E. Calleja, in *Lattice-Mismatched Thin Film*, edited by E. A. Fitzgerald (Warrendale, PA, in press).

⁹J. L. Rouviere, M. Arlery, B. Daudin, G. Feuillet, and O. Briot, *Mater. Sci. Eng., B* **50**, 61 (1997).

¹⁰L. T. Romano, J. E. Northup, and M. A. O'Keefe, *Appl. Phys. Lett.* **69**, 2394 (1996).

¹¹Z. Liliental-Weber, H. Sohn, N. Newman, and J. Washburn, *J. Vac. Sci. Technol.* **13**, 1578 (1995).

¹²J.-L. Rouviere, M. Arlery, A. Bourret, R. Niebuhr, and K. Bachem, *Inst. Phys. Conf. Ser.* **146**, 285 (1995).

¹³Z. Liliental-Weber, S. Ruvimov, Ch. Kisielowski, Y. Chen, W. Swider, J. Washburn, N. Newman, A. Gassmann, X. Lin, L. Schloss, E. R. Weber, I. Grzegory, M. Bockowski, J. Jun, T. Suski, K. Pakula, J. Baranowski, S. Porowski, H. Amano, and I. Akasaki, *Mater. Res. Soc. Symp. Proc.* **395**, 351 (1996).

¹⁴E. Calleja, M. A. Sánchez-García, D. Basak, F. J. Sánchez, F. Calle, P. Youinou, E. Muñoz, J. J. Serrano, J. M. Blanco, C. Villar, T. Laine, J. Oila, K. Saarinen, P. Hautojarvi, C. H. Molloy, D. J. Sommerford, and I. Harrison, *Phys. Rev. B* **58**, 1550 (1998).